Fifth International Symposium on Magnetic Bearings
Kanazawa, Japan, August 1996

In-situ Runout Identification in Active Magnetic Bearing System by Extended Influence Coefficient Method

Cheol-Soon Kim
Samsung Advanced Institute of Technology, P.O. Box Suwon 111, Suwon 440-600, KOREA

Chong-Won Lee
Center for Noise & Vibration Control(NOVIC), Department of Mechanical Engineering
Korea Advanced Institute of Science and Technology, Science Town, Taejon 305-701, KOREA

ABSTRACT

In this study, an efficient, yet easy to use, in-situ runout identification scheme by using extended influence coefficient method is presented for active magnetic bearing systems. Advantages of the proposed scheme are that target runout is identified and compensated under given operating condition, and it does not require any extra sensor or device for measurement of runout. It is shown experimentally that the proposed scheme successfully identifies and eliminates the troublesome runout of the AMB system in the laboratory so that a high precision spindle system can be achieved, while it is in operation.

INTRODUCTION

Active magnetic bearing(AMB) systems have drawn much attention among many researchers in rotor dynamics field, since they have been widely used in industry due to the advantages such as: free of contact and lubrication, high peripheral speed and precision operation, and adjustability of the bearing stiffness and damping up to their physical limits[1]. AMB systems always require the feedback control of magnetic force using measured displacement of rotor for stable levitation. And the positioning accuracy of an AMB system essentially depends on the quality of measured signals, which is strongly dependent upon the resolution of the sensors in use and the presence of sensing target runout. The displacement of a rotor may be measured by using non-contacting proximity measuring devices such as optical devices, eddy-current probes, capacitive probes, or inductive types. And the measured signals are affected by mechanical or electrical runout of sensing target. The mechanical runout is caused by nonconcentric rotors or surface irregularities while the electrical runout is caused by residual magnetics, metallurgical microscopic segregation or localized stress concentration[2].

The runout of sensing target in an AMB system acts as an excitation input via feedback routine, as illustrated in Fig. 1, often leading to serious rotor vibration. In Fig. 1, the measured signal contains not only the target runout but also the vibration response caused by the runout through the overall controller of the AMB system. Thus the AMB

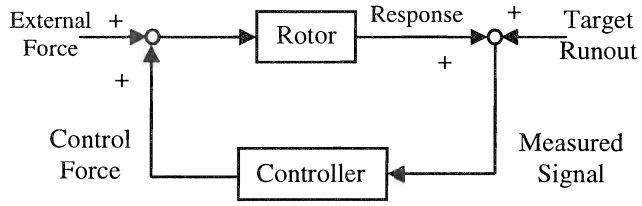

(a) Schematics of signal flow

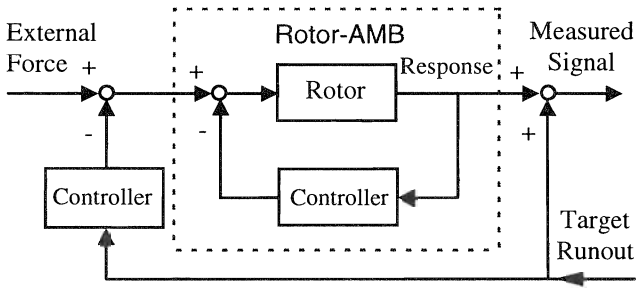

(b) Equivalent block diagram

Fig. 1 Effect of target runout in AMB system

systems used as high precision spindles require development of accurate scheme for detecting and compensating runouts[3]. Among others, Mitsui[4] investigated a measuring method of spindle rotation accuracy for precision machining based on three points method; Bifano and Dow[5] used a piezoelectric actuator to push a precision spindle against the bearing housing by measuring the master ball motion; Hara and Echigo[3] measured the runout of an ultra precision spindle supported by air bearings, using the three points method and compensated it by using AMBs.

In the previous runout compensation methods developed so far, runout identification process normally requires special arrangement for extra sensors such as a master ball or the three points method, when the rotor is not in service. But those elaborate methods can fail in accurate identification of in-situ runout, when the operating condition of interest is far different from that associated with the runout identification process, including the sensors, the

sensor locations and the operating speed.

In this study, as a new runout identification method, an in-situ runout identification scheme for AMB spindle system by using extended influence coefficient method is presented and the effect of sensing target runout on the spindle response is studied. The runout identification and compensation scheme is very similar to the open loop controller for suppressing unbalance response[6,7], except consideration of higher harmonic components as well as the fundamental harmonic component synchronous to the rotation. Advantages of the proposed scheme are that target runout is identified and compensated under a given operating condition of AMB system, and it does not require any extra sensor or device for measurement and compensation of runout.

To verify the effectiveness of the proposed runout identification scheme, experiments are performed with the laboratory AMB system, while the system is controlled by DSP-based digital controller under multi-tasking operating condition with a host-PC.

Equation of Motion with Runout

Consider the control loop for active magnetic bearing system with runout and unbalance as shown in Fig. 2: $D_o(s)$, the dynamic stiffness matrix, accounts for the inertia and gyroscopic moments of rotor and the uncontrolled magnetic bearing stiffness; $G_c(s)$ represents the transfer function matrix associated with the AMB control system; K_s is the sensor gain matrix; and $G_f(s)$ represents the electro-magnetic actuators which consist of power amplifiers and electro-magnets. The equation of motion for the controlled AMB system can be written, in Laplace domain, as

$$D_o(s)Q(s) = F_u(s) - G_f(s)G_c(s)V_e(s)$$

$$V_e(s) = K_s\{Q(s) + R(s)\} - V_{rc}(s) \qquad (1.a)$$

or

$$D_{cl}(s)Q(s) = -G_f(s)G_c(s)\{K_sR(s) - V_{rc}(s)\} + F_u(s) \qquad (1.b)$$

where

$$D_{cl}(s) = D_o(s) + G_f(s)G_c(s)K_s$$

Here Q is the displacement vector, R is the target runout vector, F_u is the unbalance force vector, V_e is the controller input vector, V_{rc} is the runout compensation signal vector; and $D_{cl}(s)$ is the dynamic matrix of the controlled AMB system. For convenient interpretation, introducing the relations

$$K_sR_c(s) \equiv V_{rc}(s)$$

we can rearrange Eq.(1.b) as

$$D_{cl}(s)Q(s) = -G_f(s)G_c(s)K_s\{R(s) - R_c(s)\} + F_u(s) \qquad (2)$$

It implies that the actual rotor motion Q is affected by runout through the controller dynamics, $G_f(s)G_c(s)K_s$, and the controlled AMB system dynamics, $D_{cl}(s)$. Note here that, once the runout R is identified, the first term in the right hand side of Eq. (2) can be easily eliminated by letting $R_c(s)=R(s)$ or setting the compensation signal as $V_{rc}(s)=K_sR(s)$. Since the true displacement, Q, can not be directly measured, and for notational convenience, a practically

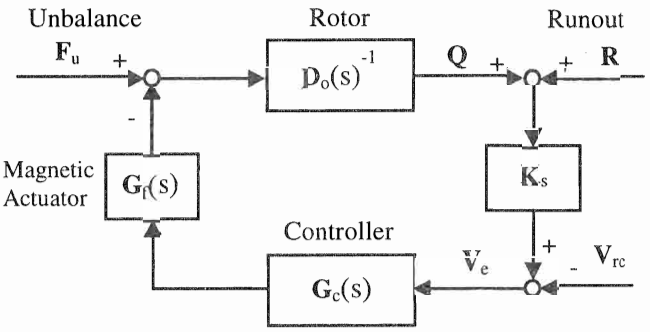

Fig. 2 Block diagram of AMB system with runout

measurable displacement, Q_e, is introduced as

$$K_sQ_e(s) \equiv V_e(s)$$

and

$$Q_e(s) = Q(s) + R(s) - R_c(s)$$

Then, we can rewrite Eq.(2) as

$$D_{cl}(s)Q_e(s) = D_o(s)\{R(s) - R_c(s)\} + F_u(s) \qquad (3)$$

Letting $s=j\omega$ and neglecting the unbalance force, $F_u(s)$, assuming that the rotor is well balanced, in Eq.(3), we obtain the expression in the frequency domain as

$$Q_e(j\omega) = H_r(j\omega)\{R(j\omega) - R_c(j\omega)\} \qquad (4)$$

where

$$H_r(j\omega) = D_{cl}(j\omega)^{-1}D_o(j\omega)$$

Here $H_r(j\omega)$ is the frequency response matrix between the measured response and the runout.

Runout Identification

Sensing target runout generates a periodic signal with the period corresponding to each rotor revolution and thus it can be represented in the form of complex Fourier series expansion as

$$r_\theta(\theta) = r_\theta(\theta + 2\pi) = \sum_{k=-\infty}^{\infty} R_{\theta k}e^{jk\theta} \qquad (5)$$

where the Fourier coefficients $R_{\theta k}$ are determined by

$$R_{\theta k} = \frac{1}{2\pi}\int_0^{2\pi} r_\theta(\theta)e^{-jk\theta}d\theta, \quad k = 0,\pm1,\pm2,...$$

Here θ is the shaft rotational angle with respect to the reference axis, y. In magnetic bearing, two identical y- and z-directional proximity sensors are located with right angle. Thus the two measured runout signals $r_y(t)$ and $r_z(t)$ are identical except the time delay with the sensor locations, i.e.

$$r_y(t) = r_\theta(\Omega t) = \sum_{k=-\infty}^{\infty} R_k e^{jk\Omega t}$$

$$r_z(t) = r_\theta\left(\Omega t - \pi/2\right) = \sum_{k=-\infty}^{\infty} R_k e^{-jk\pi/2}e^{jk\Omega t} \qquad (6)$$

where Ω is the rotational speed of the rotor and the Fourier coefficients R_k is represented by

$$R_k = \frac{\Omega}{2\pi}\int_0^{2\pi/\Omega} r_y(t)e^{-jk\Omega t}dt, \quad k = 0,\pm1,\pm2,...$$

In a typical AMB system with two radial type magnetic bearings and two measuring planes, as shown in Fig. 3, using each harmonic components, the measured response at each sensing plane due to runout becomes, from Eq.(4),

$$\boldsymbol{Q}_e(\omega_k) = \boldsymbol{H}_r(j\omega_k)\boldsymbol{R}(\omega_k) \tag{7}$$

where

$$\boldsymbol{Q}_e(\omega_k) = \begin{Bmatrix} Q_{e1k} \\ Q_{e2k} \end{Bmatrix}, \quad \boldsymbol{R}(\omega_k) = \begin{Bmatrix} R_{1k} \\ R_{2k} \end{Bmatrix}$$

$$Q_{eik} = \frac{\Omega}{2\pi}\int_0^{2\pi/\Omega} q_{ei}(t)e^{-jk\Omega t}dt, \quad k = 0,\pm1,\pm2,\ldots$$

Here Q_{eik} and R_{ik}, i=1,2 are the k-th complex Fourier coefficients of the measured signals, $q_{ei}(t)$, and the runouts taken from the i-th sensing plane, respectively.

For identification of the runout using Eq.(7), we need to first estimate the runout frequency response matrices $\boldsymbol{H}_r(j\omega_k)$ evaluated at $\omega_k=k\Omega$, k=1, 2, ... For this purpose, following two trial runout signals, r_{t1} and r_{t2}, containing N harmonic components, R_{tik}, are applied to i -th AMB at a given speed.

$$r_{ti}(t) = \sum_{k=-N}^{N} R_{tik}e^{jk\Omega t}, \quad i = 1,2 \tag{8}$$

From the three test runs at the same speed, one original and two trial runs, we can construct the following relations :

From the original test run;

$$\boldsymbol{Q}_{e0}(\omega_k) = \boldsymbol{H}_{r1}(j\omega_k)R_{1k} + \boldsymbol{H}_{r2}(j\omega_k)R_{2k} \tag{9.a}$$

For the trial runout Rt1 to AMB-1;

$$\begin{aligned}\boldsymbol{Q}_{e1}(\omega_k) &= \boldsymbol{H}_{r1}(j\omega_k)\left[R_{1k}+R_{t1k}\right]+\boldsymbol{H}_{r2}(j\omega_k)R_{2k} \\ &= \boldsymbol{Q}_{e0}(\omega_k)+\boldsymbol{H}_{r1}(j\omega_k)R_{t1k}\end{aligned} \tag{9.b}$$

For the trial runout Rt2 to AMB-2;

$$\begin{aligned}\boldsymbol{Q}_{e2}(\omega_k) &= \boldsymbol{H}_{r1}(j\omega_k)R_{1k}+\boldsymbol{H}_{r2}(j\omega_k)\left[R_{2k}+R_{t2k}\right] \\ &= \boldsymbol{Q}_{e0}(\omega_k)+\boldsymbol{H}_{r2}(j\omega_k)R_{t2k}\end{aligned} \tag{9.c}$$

where k=±1, ±2, …, N and the 2×2 influence coefficient matrix is defined from two 2×1 coefficient vector, $\boldsymbol{H}_{r1}$ and $\boldsymbol{H}_{r2}$, as

$$\boldsymbol{H}_r(j\omega_k) = \left[\boldsymbol{H}_{r1}(j\omega_k)\,|\,\boldsymbol{H}_{r2}(j\omega_k)\right]$$

Here $\omega_k=k\Omega$, k=±1,±2,··· ±N, and $\boldsymbol{Q}_{e0}$, $\boldsymbol{Q}_{e1}$ and $\boldsymbol{Q}_{e2}$ are the original response vector and the response vectors due to trial runout R_{t1} and R_{t2}, respectively. The influence coefficients are obtained from Eq. (9) as

$$\begin{aligned}\boldsymbol{H}_{r1}(j\omega_k) &= \left\{\boldsymbol{Q}_{e1}(\omega_k)-\boldsymbol{Q}_{e0}(\omega_k)\right\}/R_{t1k} \\ \boldsymbol{H}_{r2}(j\omega_k) &= \left\{\boldsymbol{Q}_{e2}(\omega_k)-\boldsymbol{Q}_{e0}(\omega_k)\right\}/R_{t2k}\end{aligned} \tag{10}$$

where $\omega_k=k\Omega$, k=±1,±2,··· ±N. Substituting the results from Eq.(10) into Eq.(9.a), we can obtain the estimate for target runout as

$$\boldsymbol{R}(\omega_k) = \begin{Bmatrix} R_{1k} \\ R_{2k} \end{Bmatrix} = \left[\boldsymbol{H}_r(j\omega_k)\right]^{-1}\boldsymbol{Q}_{eo}(\omega_k) \tag{11}$$

Finally the runout signals at each AMB can be generated from Eqs. (11) and (6). Note that the runout identification scheme explained above is very similar to the well known two plane rigid rotor balancing[8], except the consideration of higher harmonic components as well as the synchronous component.

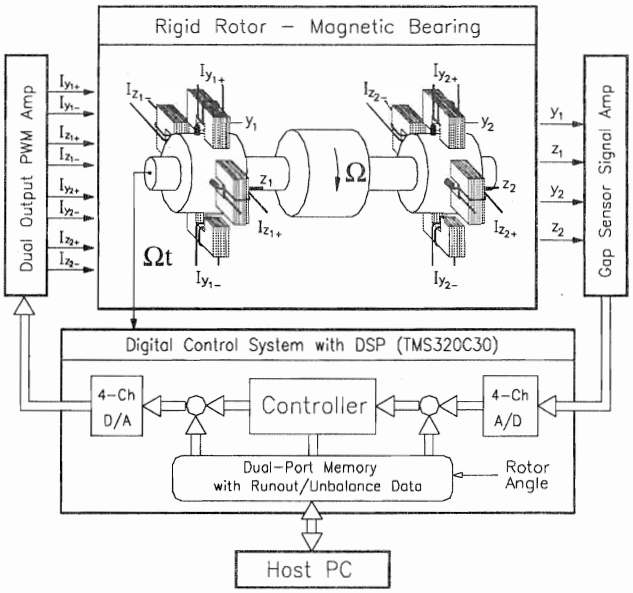

Fig. 3 Schematics of AMB system with digital controller

EXPERIMENTAL RESULT

Experimental Setup

Figure 3 shows the overall block diagram of the AMB system, which consists of a rotor, two radial magnetic bearings, four eddy current type proximity probes, a digital controller using digital signal processor(DSP) with A/D and D/A converters, four power amplifiers, a host PC and a driving motor. The rotor is composed of two magnet journals, two sensing journals and a motor armature located between two AMBs. The rotor rotational angle is measured by an incremental encoder and fed to the DSP board. The host PC is linked to DSP via dual-port memory in the DSP board, providing a multi-tasking operating condition. The PC downloads the instruction codes, control gains and runout data to DSP board, monitors the operating condition of the AMB system, and executes the runout identification procedure using transferred response signals. While the DSP performs 4-input/4-output control action and the open loop runout compensation. For the tested AMB system shown, the rotor mass is 8.34kg, the bearing span length is 277 mm, and the diameter of the magnet and sensing journal is 89 mm.

Runout Estimation Result

In order to estimate the influence coefficients defined in Eqs. (9) and (10), two trial runout signals containing 30 harmonic components were input to the DSP memory and the resulting responses were captured by the host PC. During the test, the control gains and the rotational speed remained unchanged. Since the sampled data are essentially periodic

with the period of one revolution, rotation angle based discrete complex Fourier transformation of the measured signals was performed. Then the complex Fourier coefficients of the runout calculated from Eq. (11) were substituted into Eq.(6), in order to generate the estimated runout signals in the time domain. Finally the runout signals were loaded to the DSP memory to measure the runout compensated responses.

Figures 4 shows the measured responses at each AMB when the AMB system was run at 2000rpm without runout compensation. Here the y- and z-directional responses are very similar only with the 90 degrees phase difference, which is owing to the isotropic control of AMB system[9]. Note that the response at AMB-1 is dominated by the second harmonic component and that the response at AMB-2 has the magnitude less than 10μm and the wide frequency band.

Figures 5 is the identified runout signals at each AMB at 2000rpm. The estimated runout at AMB-1, as shown in Fig. 5(a), is mainly composed of the first and second harmonic components. It indicates that the presence of a short duration spike in the responses shown in Fig.4(a) is due to the runout at AMB-1. The estimated runout at AMB-2 shown in Fig. 5(b) is also dominated by the first and second harmonics, but their amplitudes are far smaller than those of AMB-1.

Figure 6 shows the actual vibration response of the AMB rotor at 2000rpm due to the target runouts, which is obtained by subtracting the estimated runout signals shown in Fig. 5 from the measured responses shown in Fig. 4. Comparison of Figs. 4 and 6 indicates that the runout signal tends to cause serious response at 2000 rpm. In fact, it was found that the second harmonic component of runout is fed back through the control loop of the AMB system and it excites the fundamental resonant mode at 74 Hz of the rotor-AMB system.

Figure 7 shows the measured whirl responses of the AMB system at 2000 rpm after runout compensation using the estimated runouts shown in Fig. 5. It clearly evidences that the target runouts were effectively identified and removed, resulting in that the runout compensated signals remained within the sensor resolution of 0.5μm.

Finally, it was shown that the proposed runout estimation scheme is very efficient and simple to use, only requires three test runs and a signal processing. While the runout estimation process is performed without rotor stop and takes less than one minute, including data acquisition time.

CONCLUSION

The effect of sensing target runout on the rotor response is formulated for active magnetic bearing system and an efficient, yet easy to use in-situ runout identification scheme by extended influence coefficient method is proposed. The experimental results show that the proposed scheme works excellently with the laboratory AMB system.

REFERENCES

1. Brunet, M., 1988, "Practical Applications of the Magnetic Bearings to the Industrial World," 1st International Symposium on Magnetic Bearings, Zurich, pp. 225-244.
2. Bently Nevada Corporation, 1979, "Vector Nulling versus Runout Compensation," Application Note, No. L0196.
3. Hara, S., and Echigo, K., 1992, "A Trial Product of Ultra Precision Spindle," 3rd International Symposium on Magnetic Bearings, Alexandria, pp. 421-428.
4. Mitsui, K., 1992, "Development of New Measuring Method for Spindle Rotating Accuracy by Three Points Method," Proceedings of 23rd International MTDR Conference, pp.195-121.
5. Bifano, T. G., and Dow, T. A., 1985, "Real Time Control of Spindle Runout," Optical Engineering, Vol.34, No. 5, pp. 888-892.
6. Higuchi, T., Otsuka, M., Mizuno, T., and Ide, T., 1990, "Application of Periodic Learning Control with Inverse Transfer Function Compensation in Totally Active Magnetic Bearings," 2nd International Symposium on Magnetic Bearings, Tokyo, pp. 257-264.
7. Knospe, C. R., Hope, R. W., Fedigan, S. J., and Williams, R. D., 1993, "Adaptive On-Line Rotor Balancing Using Digital Control," Proceedings of MAG93 Magnetic Bearings, Magnetic Drives, and Dry Gas Seals Conference, Alexandria, pp. 153-164.
8. Lee, C. W., 1993, *Vibration Analysis of Rotors*, Kluwer Academic Publishers, pp. 215-221.
9. Kim, C.S. and Lee, C. W., 1994, "Isotropic Optimal Control of Active Magnetic Bearing System," 4th International Symposium on Magnetic Bearings, Zurich, pp.35-40.

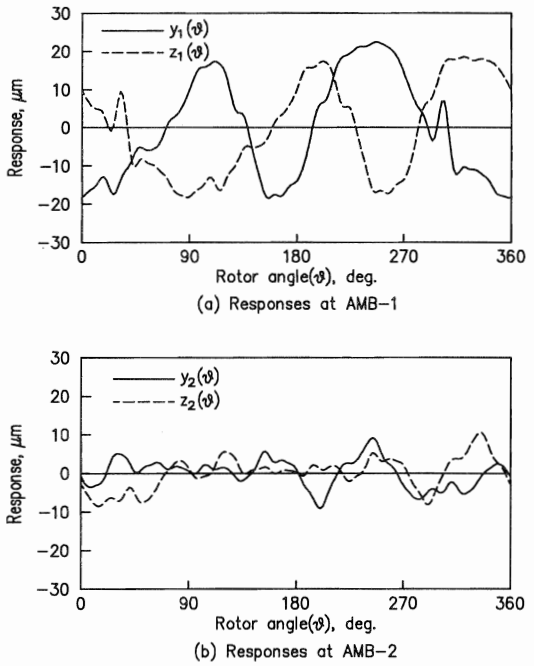

Fig. 4 Measured responses of AMB system at 2000rpm without runout compensation

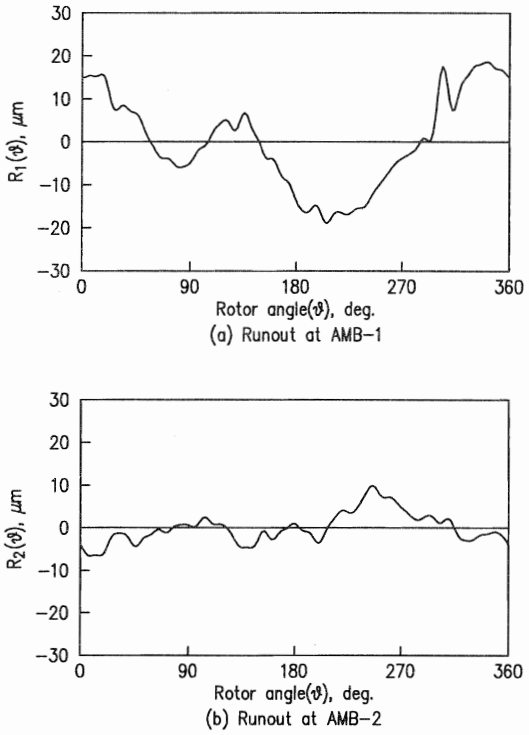

Fig. 5 Estimated target runouts of AMB at 2000rpm

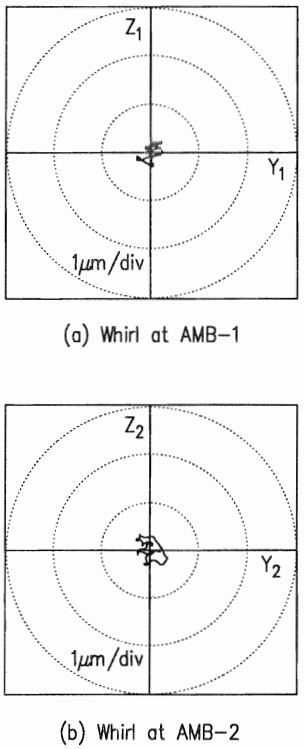

Fig. 7 Whirl of AMB with runout compensation at 2000rpm

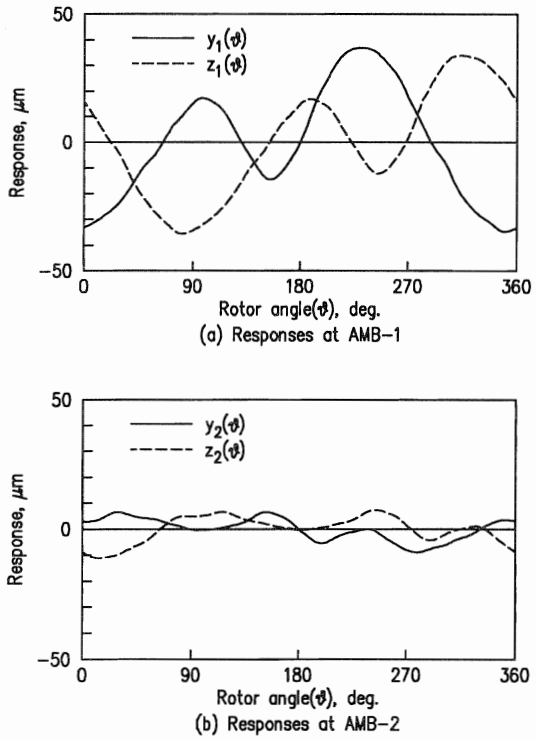

Fig. 6 Actual responses of AMB system at 2000rpm due to target runouts